

# Rheologically tuned diffusion modulates quorum sensing in *Vibrio fischeri*

Chunhe Li, Zixiang Lin, Hongyi Bian, Anqi Li, Hongyi Xin, Zijie Qu

## Abstract

Understanding how the physical properties of a fluid influence bacterial behavior is essential for explaining how microorganisms interact with their environment and with animal hosts. Here, we examine how changes in fluid viscosity and rheological properties affect the locomotion of the marine bacterium *Vibrio fischeri* and its ability to produce luminescence through cell-cell communication. We track the three-dimensional motion of single cells in well-defined fluids with different physical properties and measure the luminescence emitted by cell populations. We find that fluids with higher viscosity cause *V. fischeri* to spend more time in a slower, turning-focused swimming mode, which reduces how effectively cells spread out and encounter the chemical signals required to activate luminescence. As a result, luminescence first increases and then decreases in Newtonian fluids, but decreases monotonically in fluids that exhibit non-Newtonian rheological behavior. Computer simulations based on our measurements confirm that the ability of cells to explore their surroundings plays a central role in determining when and how strongly they communicate. These findings reveal a direct link between the physical environment, bacterial movement, and collective behavior, and offer new insight into how microorganisms adapt to complex fluid habitats, including those found inside animal hosts.

## 1 Introduction

Microorganisms inhabit physically diverse liquid environments in which the physical properties of the surrounding fluid strongly influence their ability to navigate, sense, and communicate across multiple spatial and temporal scales [1–4]. Viscosity, elasticity, and shear-thinning behavior shape not only the hydrodynamic forces experienced by swimming cells but also the transport [5, 6], accumulation [7], and perception of signaling molecules that coordinate collective behaviors [8, 9]. Such physical constraints are ubiquitous in natural habitats, including marine snow [10, 11], host mucus layers [12, 13], and polymer-rich biological secretions, where fluids frequently deviate from Newtonian behavior and exhibit complex rheological responses [14, 15]. Understanding how environmental rheology regulates cellular locomotion and chemical communication is therefore essential for linking microscopic motility to ecological and host-associated functions.

A compelling illustration of the ecological relevance of fluid–cell interactions is the binary symbiosis between *Vibrio fischeri* and the Hawaiian bobtail squid, *Euprymna scolopes* [16–18]. Newly hatched squid depend on motile *V. fischeri* cells to traverse a heterogeneous, mucus-rich landscape and reach the light organ, where successful colonization requires cells to accumulate, persist, and communicate within spatially confined crypts [19–21]. Within these microenvironments, the buildup of autoinducer molecules activates quorum sensing (QS), triggering bioluminescence that enables the squid’s nocturnal counterillumination [22, 23]. Schematic of quorum-sensing (QS) regulation in *V. fischeri* is shown in Fig. 1. This iconic symbiosis thus exemplifies how bacterial motility, environmental physical properties, and QS activation are tightly coupled, yet the physical principles governing this coupling remain incompletely understood.

Previous studies have established that bacterial motility is highly sensitive to fluid rheology. In Newtonian fluids, increased viscosity generally reduces swimming speed by enhancing hydrodynamic drag [24–27]. In contrast, dilute polymer solutions can produce non-intuitive responses: for example, *E. coli* has been reported to swim faster in certain shear-thinning polymer solutions, in contrast to its behavior in Newtonian fluids [28–30]. These findings demonstrate that the impact of complex fluids on bacterial locomotion is species-specific and depends on cell morphology, flagellar architecture, and motor regulation. Despite extensive work on the QS circuitry and ecological role of *V. fischeri*, how

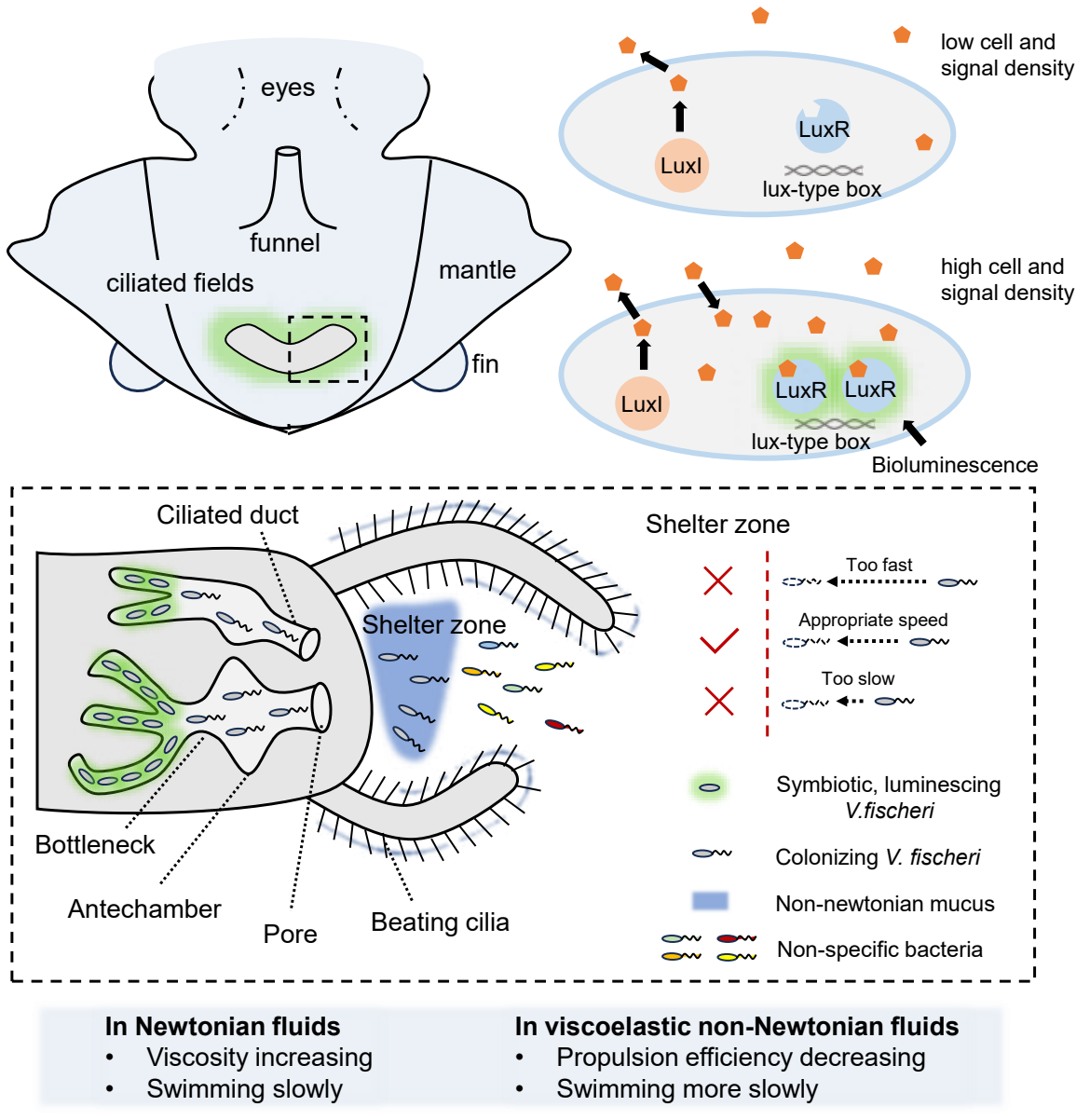


Figure 1: Schematic of quorum-sensing (QS) regulation in *V. fischeri*. At low cell and signal density, LuxR remains inactive; accumulation of autoinducer molecules at high density activates LuxR binding to the lux-type box, triggering bioluminescence. Conceptual model of *V. fischeri* colonization in the light organ of the Hawaiian bobtail squid (*Euprymna scolopes*). Beating cilia transport bacteria toward the light-organ ducts while secreting non-Newtonian mucus. Bacteria with swimming speeds that are too fast or too slow are inefficiently captured, whereas an appropriate swimming speed promotes entry into the shelter zone and successful colonization. Increased viscosity and viscoelasticity reduce propulsion efficiency, leading to slower swimming in non-Newtonian fluids, consistent with the experimentally observed motility reduction and its impact on QS-mediated bioluminescence. Illustration of bacterial space exploration characterized by different effective diffusion coefficients. Larger effective diffusion coefficients correspond to more efficient exploration and higher encounter rates between cells and signal molecules.

its motility responds to non-Newtonian, mucus-like environments—and how such responses feed back into QS-mediated behaviors—remains largely unexplored.

A distinctive feature of *V. fischeri* is its polymorphic swimming behavior, characterized by run–reverse and run–pause–reverse modes enabled by a flagellar wrapping mechanism [31, 32]. These swimming modes generate large reorientation angles and strongly influence how efficiently cells explore confined or structured spaces [33, 34]. Because QS activation depends on the accumulation of signal molecules over time, the long-time effective diffusion of a bacterial population, rather than instantaneous swimming speed alone, is likely to govern the onset and spatial organization of bioluminescence [29, 35, 36]. However, how this diffusion-like behavior emerges from viscosity-dependent swimming dynamics, particularly under viscoelastic stresses, has not been experimentally quantified.

Here, we investigate how fluid rheological properties regulate both swimming behavior and QS-mediated bioluminescence in *V. fischeri*. Using Newtonian solutions of poly(vinylpyrrolidone) (pvp;  $M_w \approx 360$  kDa, denoted as PVP360k) and non-Newtonian solutions of shear-thinning, viscoelastic methylcellulose (Methocel), we combine real-time three-dimensional tracking of individual cells with population-level measurements of QS-driven luminescence. By quantifying motility-mode fractions, run durations, reorientation statistics, and swimming speeds across a range of viscosities, we derive the effective diffusion coefficient of *V. fischeri* and directly link it to QS activation. Complementary simulations coupling bacterial motion with viscosity-dependent molecular diffusion reproduce the observed luminescence trends, revealing how fluid rheology modulates collective bacterial signaling through its impact on long-time transport statistics. Together, our results identify effective diffusion as a physical bridge between single-cell motility and QS-controlled symbiotic function.

## 2 Results and Discussion

### 2.1 Effect of Liquid Viscosity on QS-Mediated Bioluminescence

To investigate how fluid rheological properties influence quorum-sensing (QS)-regulated bioluminescence in *V. fischeri*, we systematically tune the physical properties of the surrounding medium using PVP360k, which maintains the medium as a Newtonian fluid, and Methocel, which introduces shear-thinning and viscoelastic behavior (rheological properties shown in the SI). We then examine changes in bioluminescence intensity for bacterial suspensions at fixed cell concentration under different viscosities. Cells cultured for more than 24 h are harvested, centrifuged, and resuspended in motility buffer at a fixed cell concentration (details shown in the SI). The vial is placed in a dark chamber, and a color camera records the bioluminescence intensity and duration by continuous imaging.

We find that the viscosity-dependent response of bioluminescence differs qualitatively between Newtonian and non-Newtonian liquids (Fig. 2A). For bacteria suspended in motility buffer containing PVP360k, the bioluminescence intensity increases and then decreases with increasing viscosity, reaching a maximum at a viscosity of 1.5 cP. In contrast, for bacteria in motility buffer containing Methocel, the mean luminescence decreases monotonically with viscosity. Fig. 2B and 2C show the temporal evolution of the mean intensity in the luminescent region. The average luminescence intensity depends on both the viscosity and the rheological properties of the motility buffer, whereas the overall duration of bioluminescence is independent of these factors. In both PVP360k- and Methocel-containing buffers, bioluminescence decays slowly during the first 7–8 min of observation and drops to its minimum level after approximately 13 min. This distinct viscosity-dependent modulation of luminescence intensity motivates us to further examine the swimming behavior of individual *V. fischeri* cell.

### 2.2 Effect of Complex Fluids on the Swimming Speed of *V. fischeri*

We measure and analyze the swimming behavior of *V. fischeri* in motility buffers with different fluid properties using a real-time 3D tracking microscope [27]. As shown in Fig. 3, each individual cell is tracked for 10 s. In motility buffer supplemented with PVP360k, the mean swimming speed decreases monotonically with increasing viscosity, consistent with expectations for Newtonian fluids. To elucidate the origin of this viscosity-dependent slowdown, we further examine the motility modes of individual cells. *V. fischeri* exhibits pronounced “run–reverse” and “run–pause–reverse” behaviors, corresponding to the push–pull and push–wrap–pull swimming modes [31, 32], respectively. As illustrated in Fig. 3A, entry into the wrap mode is accompanied by a substantial reduction in instantaneous swimming speed

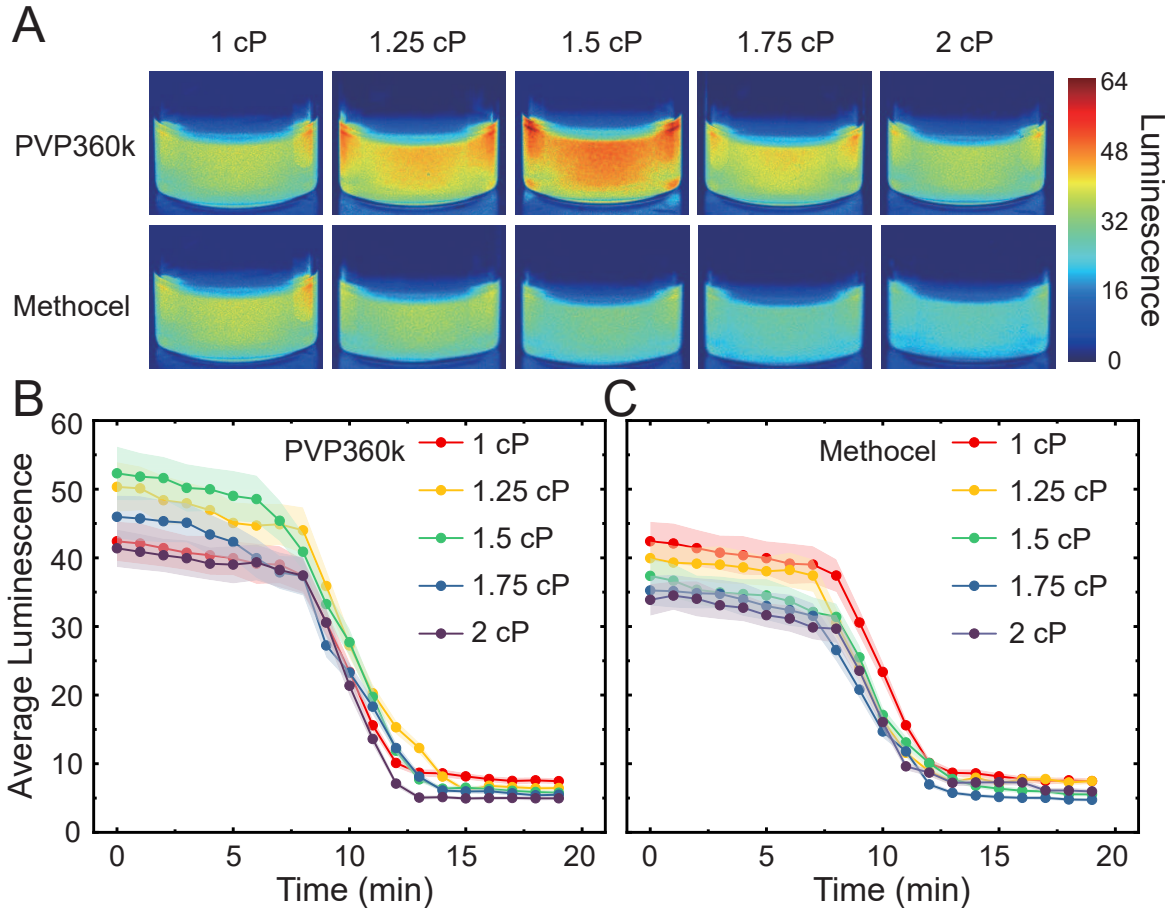


Figure 2: Viscosity-dependent modulation of quorum-sensing-mediated bioluminescence in *V. fischeri*. (A) Representative false-color images of bioluminescence intensity for bacterial suspensions at fixed cell concentration in motility buffers containing PVP360k (Newtonian fluid, top row) and Methocel (shear-thinning viscoelastic fluid, bottom row) at different viscosities. Color scale indicates luminescence intensity. Temporal evolution of the spatially averaged luminescence intensity in PVP360k (B) and Methocel (C) containing motility buffer for viscosities ranging from 1 to 2 cP. The solid points represent the average intensity, while the shaded areas represent the standard deviation. The mean luminescence intensity exhibits a nonmonotonic dependence on viscosity, with a maximum at intermediate viscosity.

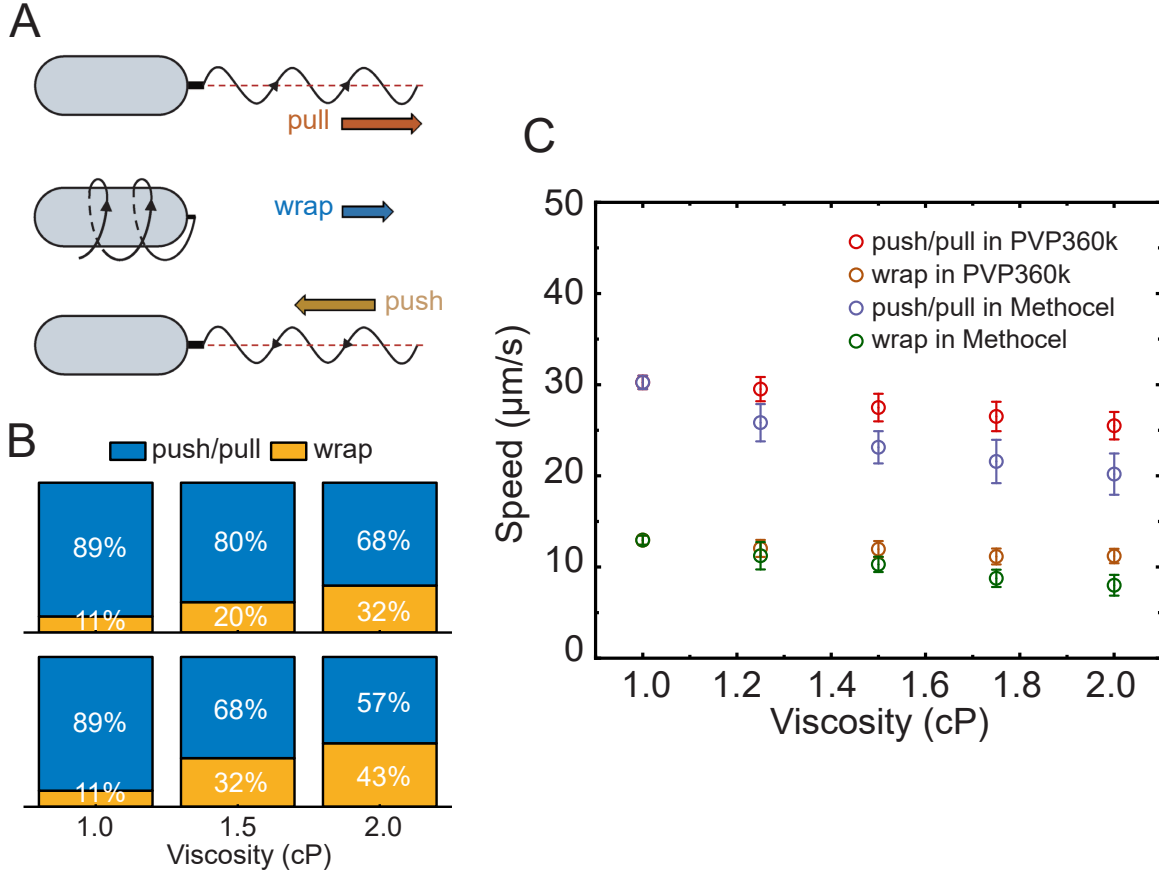


Figure 3: Motility modes and viscosity-dependent swimming behavior of *V. fischeri* in Newtonian and non-Newtonian fluids. (A) Schematic illustration of the three characteristic motility modes of *V. fischeri*: push, pull, and wrap. Push and pull modes correspond to straight swimming driven by flagellar rotation, whereas the wrap mode arises from flagellar bundling around the cell body and is associated with reduced propulsion efficiency. (B) Fraction of trajectories exhibiting push/pull and wrap modes at selected viscosities. The upper panel shows data obtained in PVP360k-containing Newtonian fluids, whereas the lower panel corresponds to Methocel-containing viscoelastic fluids. (C) Swimming speed as a function of viscosity for different motility modes in motility buffers containing PVP360k (Newtonian fluid) and Methocel (shear-thinning viscoelastic fluid).

compared to the push and pull modes. We therefore segment the three-dimensional trajectories to quantify both the fraction of time spent in each motility mode and the corresponding mode-resolved swimming speeds across different viscosities.

As shown in Fig. 3B, the probability of the wrap mode increases systematically with viscosity in both PVP360k and Methocel-containing buffers. This trend is consistent with previous studies, where increased viscous resistance promotes the occurrence of flagellar wrapping events [37]. However, in contrast to earlier studies on *Escherichia coli* [28–30], *V. fischeri* does not exhibit enhanced swimming speed with increasing viscosity in shear-thinning fluids. Fig. 3C shows that swimming speeds decrease in both the straight swimming modes (push and pull) and the wrap mode. Specifically, for the same viscosity, swimming speeds in Methocel solutions are lower than in the Newtonian PVP360k solution, whether in the straight swimming modes (push and pull) or the wrapping mode.

### 2.3 Relationship between the Diffusion and Bioluminescence

Previous studies indicate that quorum sensing in *V. fischeri* is activated once cells encounter a sufficiently high local concentration of signal molecules, leading to the onset of bioluminescence [38, 39]. This suggests that the efficiency with which cells explore their surroundings plays a key role in QS

activation, and can be quantitatively characterized by an effective diffusion coefficient  $D$  [29, 40]. The swimming behavior of *V. fischeri* consists of straight runs at speed  $v$ , intermittently interrupted by reorientation events associated with flagellar wrapping and unwrapping. These reorientation events are characterized by a run duration  $\tau_{\text{run}}$ , a wrapping time  $\tau_{\text{wrap}}$ , and a turning angle  $\theta$  (Fig. 4A). Analysis of the trajectory statistics shows that the distribution of run durations is well described by an exponential form (Fig. 4C, inset), supporting a Poisson description of reorientation events [41]. In addition, the wrapping duration  $\tau_{\text{wrap}}$  is consistently much shorter than the corresponding run time  $\tau_{\text{run}}$  across all viscosities (Fig. 4B and C). The mean turning angle decreases systematically with increasing  $\tau_{\text{wrap}}$ , and the dependence is well captured by an exponential fit for both PVP360k- and Methocel-containing buffers (Fig. 4B), indicating that longer wrapping events lead to more persistent swimming directions [34].

Using the measured three-dimensional trajectories, we extract  $v$ ,  $\tau_{\text{run}}$ , and the turning-angle statistics at each viscosity for both motility buffers. Both the mean run duration and the mean turning angle decrease monotonically with increasing viscosity in PVP360k and Methocel solutions (Fig. 4B and C). The ability of bacteria to explore the  $D = v^2 \tau_{\text{run}} / 3(1 - \langle \cos \theta \rangle)$  [41]. Substituting these measured quantities into equation yields the effective diffusion coefficient  $D$ . As shown in Fig. 4D,  $D$  exhibits a nonmonotonic dependence on viscosity in PVP360k containing Newtonian fluids, whereas it decreases monotonically with viscosity in Methocel containing viscoelastic fluids.

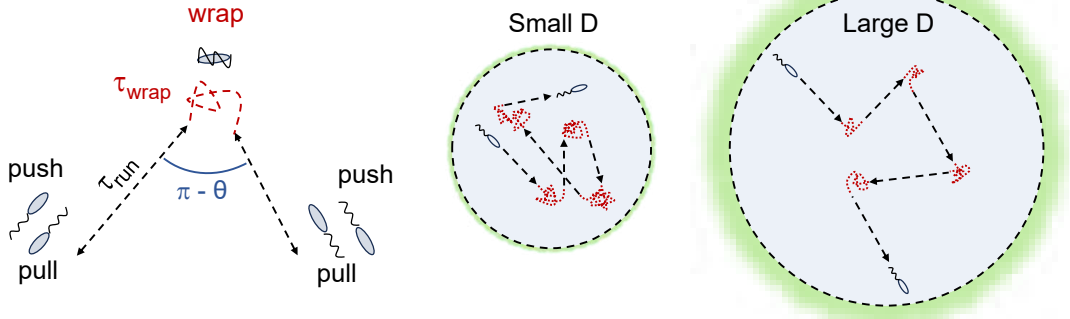
To connect these transport properties to QS activity, we quantify the mean bioluminescence intensity during the emission period for cell populations at identical concentration. The viscosity dependence of the luminescence intensity closely mirrors that of the effective diffusion coefficient for both motility buffers (Fig. 4D and E). We employ a simplified diffusion-based model to simulate the interaction between *V. fischeri* cells and surrounding signal molecules under representative experimental conditions (16°C) in a confined domain of 300  $\mu\text{m} \times 300 \mu\text{m}$ . In this model, the active motion of the cells is described by the effective diffusion coefficients measured at different viscosities in the two motility buffers, while the passive motion of signal is modeled using the viscosity-dependent diffusion coefficients of small molecules. The normalized number of signal-cell encounter events is used to quantify the luminescence intensity. As shown in Fig. 4E, the simulations reproduce the overall experimental trends. Together, these results indicate that the “searching efficiency” of the cells, quantified by the effective diffusion coefficient, constitutes a key physical factor linking motility statistics to QS-activated bioluminescence.

### 3 Conclusion

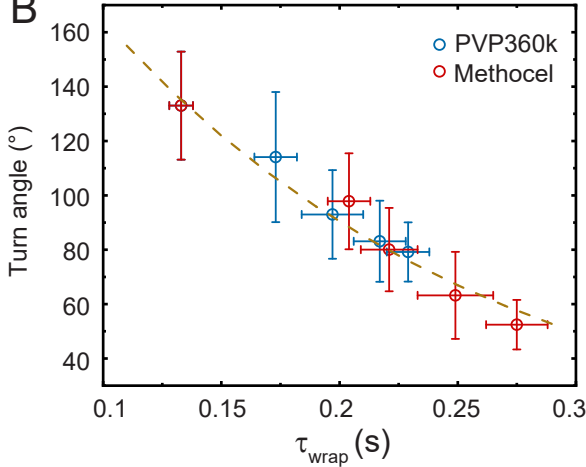
In this work, we examine how liquid viscosity and fluid rheology regulate quorum-sensing (QS)-mediated bioluminescence in *V. fischeri*, under the hypothesis that viscosity-dependent changes in bacterial motility—rather than viscosity alone—govern the efficiency of signal encounter and accumulation. By systematically comparing Newtonian and shear-thinning viscoelastic fluids, we aim to establish a physical link between microbial transport, motility modes, and QS activation learned from experiments and modeling. Our results reveal that fluid rheology plays a decisive role in shaping QS-regulated bioluminescence. In Newtonian fluids, the luminescence intensity exhibits a nonmonotonic dependence on viscosity, whereas in viscoelastic Methocel solutions it decreases monotonically. Single-cell tracking demonstrates that increasing viscosity improves the probability of flagellar wrapping and restricts swimming speed, with viscoelastic stresses further amplifying this reduction. Unlike previously reported viscosity-enhanced motility in *E. coli*, *V. fischeri* shows no speed enhancement in shear-thinning media, underscoring the importance of species-specific motility mechanisms and flagellar dynamics. Considering that this is a phenomenon worth investigating, but not the main focus of our current work, we will conduct detailed experimental and theoretical studies on the speed reduction behavior of *V. fischeri* in viscoelastic fluids in future work.

Importantly, these findings resonate with the natural symbiotic context of *V. fischeri* and the Hawaiian bobtail squid *Euprymna scolopes*. During the initial colonization process, ciliary beating on the squid light-organ surface captures bacteria from seawater while simultaneously secreting mucus that is known to exhibit non-Newtonian, viscoelastic properties. Previous studies show that bacterial swimming speeds that are either too high or too low reduce capture and retention efficiency by the host [42, 43]. Our observation that *V. fischeri* experiences a pronounced motility slowdown in non-Newtonian fluids therefore aligns with this ecological constraint, suggesting that fluid rheology may act

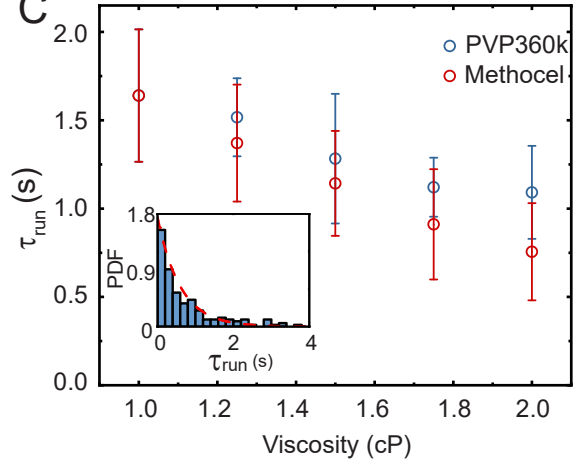
A



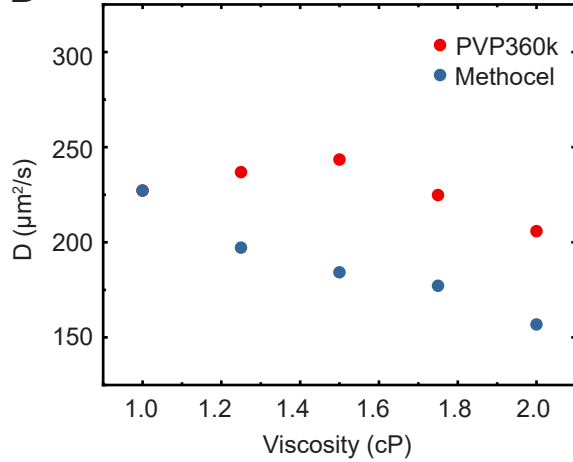
B



C



D



E

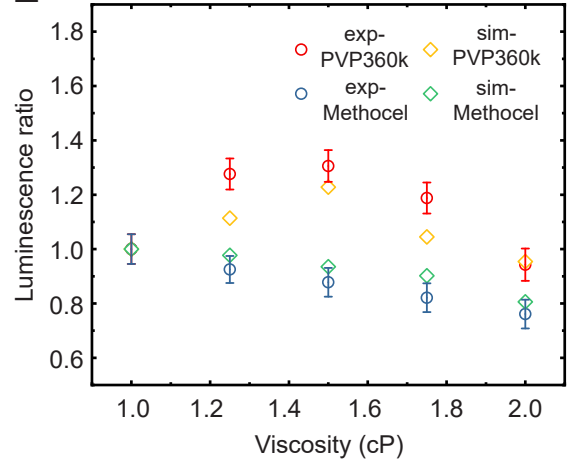


Figure 4: Motility statistics, effective diffusion, and their connection to quorum-sensing activity in *V. fischeri*. (A) Schematic illustration of the motility statistics used to characterize cell reorientation and environmental exploration. Straight swimming in push and pull modes is intermittently interrupted by wrap events of duration  $\tau_{\text{wrap}}$ , leading to a reorientation characterized by the turning angle  $\theta$  and an effective run duration  $\tau_{\text{run}}$ . Representative trajectories illustrate how different motility statistics give rise to smaller or larger effective diffusion coefficients  $D$ . (B) Mean turning angle as a function of the wrap duration  $\tau_{\text{wrap}}$  for cells swimming in PVP360k- and Methocel-containing motility buffers. Dash line represents exponential fits to the data. (C) Mean run duration  $\tau_{\text{run}}$  as a function of viscosity. Inset: probability density function (PDF) of run durations with an exponential fit, supporting a Poisson description of reorientation events. (D) Effective diffusion coefficient  $D$  calculated from the measured swimming speed, run duration, and turning-angle statistics. (E) Comparison between the normalized mean luminescence intensity measured experimentally and simulation results based on a diffusion-controlled interaction model between cells and signal molecules.

as a physical regulator that tunes bacterial transport during host-mediated selection and accumulation.

By quantifying swimming speed, turning angles, and motility-mode fractions, we derive an effective diffusion coefficient that characterizes how efficiently cells explore their environment. We show that the viscosity-dependent variation of this diffusion coefficient consistently predicts the observed changes in luminescence intensity across both Newtonian and non-Newtonian fluids. A diffusion-based interaction model between cells and signal molecules further reproduces the experimental trends, highlighting “search efficiency” as a key physical control parameter linking hydrodynamic transport to collective biochemical activation.

Several limitations of this study should be acknowledged. The effective diffusion description of active particles short-time motility dynamics neglects potential biochemical feedback between QS activation and motility. In addition, rheological parameters are taken from bulk measurements and may not fully capture local responses of the near-flagellum fluid. Finally, the model considers a simplified confined geometry and does not explicitly account for cell–cell interactions or heterogeneous signal production. Future work may address these limitations by coupling intracellular QS regulation to motility dynamics, probing near-field viscoelastic effects at the single-flagellum scale, and extending the framework to higher cell densities or structured environments. Exploring how fluid rheology modulates QS in other motile bacteria may reveal further the general physical principles that govern microbial communication.

## 4 Acknowledgments

We thank Yu Cheng and Jin Zhu for the comments and discussions on the paper content. Our work is funded by National Natural Science Foundation of China (NSFC), Grant No. 12202275, and Shanghai Jiao Tong University Explore X Grant.

## References

- [1] K. V. S. Chaithanya et al. Viscoelastic effects on the hydrodynamics of an active swimmer. *Physics of Fluids*, 37(5):1–20, 2025.
- [2] G. J. Elfring and E. Lauga. Theory of locomotion through complex fluids. *Journal of Fluid Mechanics*, 758:1–29, 2014.
- [3] E. Lauga. Bacterial hydrodynamics. *Annual Review of Fluid Mechanics*, 48:29–51, 2016.
- [4] Y. Quan et al. The locomotion of microorganisms in viscoelastic fluids at finite reynolds numbers. *Journal of Fluid Mechanics*, 898:1–34, 2025.
- [5] V. Wong et al. Fluid flow structures gut microbiota biofilm communities by advective transport of molecules. *Proceedings of the National Academy of Sciences*, 120(42):e2217577120, 2023.
- [6] M. Winkle et al. Signaling in microbial communities with open boundaries. *Nature Communications*, 14:10397789, 2023.
- [7] C. Scheidweiler et al. Spatial structure, chemotaxis and quorum sensing shape bacterial biomass accumulation in complex porous media. *Nature Communications*, 15:44267, 2024.
- [8] D. Cornforth et al. Combinatorial quorum sensing allows bacteria to resolve complex environments. *Proceedings of the National Academy of Sciences*, 111(50):18356–18361, 2014.
- [9] M. Boyer et al. Cell–cell signalling in bacteria: not simply a matter of quorum. *FEMS Microbiology Ecology*, 70(1):1–10, 2009.
- [10] L. Gram et al. Possible quorum sensing in marine snow bacteria. *Environmental Microbiology*, 4(6):405–409, 2002.
- [11] E. Bar-Zeev and H. Dang. Microbial surface colonization and biofilm development in marine aggregates. *Marine Environmental Research*, 114:39–47, 2016.

- [12] M. Lai et al. Micro- and macrorheology of mucus. *Annual Review of Fluid Mechanics*, 41:123–145, 2009.
- [13] M. Mrokowski et al. Effect of exopolymer gels on the viscoelasticity of mucus-rich saltwater and settling dynamics of particles. *Science of the Total Environment*, 813:151681, 2022.
- [14] U. Passow. The origin of transparent exopolymer particles (tep) and their role in the sedimentation of particulate matter. *Deep Sea Research Part II: Topical Studies in Oceanography*, 48(8-9):2415–2438, 2001.
- [15] Various authors. The biology of mucus: Composition, synthesis and organization. *Nature Reviews Molecular Cell Biology*, 24(4):234–250, 2023.
- [16] S. V. Nyholm, E. V. Stabb, E. G. Ruby, and M. J. McFall-Ngai. Establishment of an animal–bacterial association: recruiting symbiotic vibrios from the environment. *Proceedings of the National Academy of Sciences*, 97(18):10231–10235, 2000.
- [17] J. C. Nawroth, H. Guo, E. Koch, E. A. C. Heath-Heckman, J. C. Hermanson, E. G. Ruby, J. O. Dabiri, E. Kanso, and M. J. McFall-Ngai. Motile cilia create fluid-mechanical microhabitats for the active recruitment of the host microbiome. *Proceedings of the National Academy of Sciences*, 114(36):9510–9516, 2017.
- [18] S. V. Nyholm and M. J. McFall-Ngai. Dominance of *vibrio fischeri* in secreted mucus outside the light organ of *euprymna scolopes*: the first site of symbiont specificity. *Applied and Environmental Microbiology*, 69(7):3932–3937, 2003.
- [19] Spencer V. Nyholm and Margaret J. McFall-Ngai. A lasting symbiosis: how the hawaiian bob-tail squid finds and keeps its bioluminescent bacterial partner. *Nature Reviews Microbiology*, 19(10):666–677, 2021.
- [20] Katrina A. Gundlach, Janna Nawroth, Eva Kanso, Farzana Nasrin, Edward G. Ruby, and Margaret McFall-Ngai. Ciliated epithelia are key elements in the recruitment of bacterial partners in the squid-vibrio symbiosis. *Frontiers in Cell and Developmental Biology*, 10:974213, 2022.
- [21] Alba Chavez-Dozal, David A. Hogan, Clayton Gorman, Alvaro Quintanal-Villalonga, and Michele K. Nishiguchi. Multiple *\*vibrio fischeri\** genes are involved in biofilm formation and host colonization. *FEMS Microbiology Ecology*, 81(3):562–573, 2012.
- [22] J. Engebrecht, K. Nealson, and M. Silverman. Identification of genes and gene products necessary for bacterial bioluminescence. *Proceedings of the National Academy of Sciences*, 81(13):4154–4158, 1984.
- [23] C. Fuqua, S. C. Winans, and E. P. Greenberg. Quorum sensing in bacteria: the *\*luxr-luxi\** family of cell density responsive transcriptional regulators. *Annual Review of Microbiology*, 50:727–751, 1996.
- [24] Bo Qin, Arvind Gopinath, Jing Yang, Menachem Elimelech, and Paulo E. Arratia. Flagellar kinematics and swimming of algal cells in newtonian and viscoelastic fluids. *Scientific Reports*, 5:9190, 2015.
- [25] J. B. Keller. Effect of viscosity on swimming velocity of bacteria. *Proceedings of the National Academy of Sciences*, 71(8):3253–3253, 1974.
- [26] Eric Lauga and Thomas R. Powers. The hydrodynamics of swimming microorganisms. *Reports on Progress in Physics*, 72(9):096601, 2009.
- [27] Zijie Qu, Fatma Zeynep Temel, Rene Henderikx, and Kenneth S. Breuer. Changes in the flagellar bundling time account for variations in swimming behavior of flagellated bacteria in viscous media. *Proceedings of the National Academy of Sciences*, 115(8):1707–1712, 2018.
- [28] Zijie Qu and Kenneth S. Breuer. Effects of shear-thinning viscosity and viscoelastic stresses on flagellated bacteria motility. *Physical Review Fluids*, 5(7):073103, 2020.

- [29] Alison E. Patteson, Arvind Gopinath, Mark Goulian, and Paulo E. Arratia. Running and tumbling with *E. coli* in polymeric solutions. *Scientific Reports*, 5:15761, 2015.
- [30] Andreas Zöttl and Julia M. Yeomans. Enhanced bacterial swimming speeds in macromolecular polymer solutions. *Nature Physics*, 15:554–558, 2019.
- [31] Jonathan B. Lynch et al. Transitioning to confined spaces impacts bacterial swimming and escape response. *Biophysical Journal*, 122(x):xx–xx, 2022.
- [32] Yoshiaki Kinoshita, Yoshitomo Kikuchi, Nagisa Mikami, Daisuke Nakane, and Takayuki Nishizaka. Unforeseen swimming and gliding mode of an insect gut symbiont, *burkholderia* sp. rpe64, with flagella wrapping around its cell body. *The ISME Journal*, 12(3):838–848, 2018.
- [33] R. Stocker, J.R. Seymour, A. Samadani, D.E. Hunt, and M.F. Polz. Rapid chemotactic response enables marine bacteria to exploit ephemeral microscale nutrient patches. *Proceedings of the National Academy of Sciences*, 105(11):4209–4214, 2008.
- [34] Ming Tian, Wenchao Zhu, Ruisong Xu, Mao Liu, Ji Yuan, Lijuan Jiang, Jiao Yuan, and Jing Yuan. A new mode of swimming in singly flagellated *pseudomonas aeruginosa*. *Proceedings of the National Academy of Sciences*, 119(16):e2120508119, 2022.
- [35] A. Villa-Torrealba, C. Chávez-Raby, P. de Castro, and R. Soto. Run-and-tumble bacteria slowly approaching the diffusive regime. *Physical Review E*, 101(6):062607, 2020.
- [36] G. Guccione et al. Diffusivity of *e. coli*-like microswimmers in confined geometries. *Physical Review E*, 96(4):042603, 2017.
- [37] Xiang Yu Zhuang, Chao Kai Tseng, and Chien Jung Lo. Viscosity-dependent swimming patterns assist *aliivibrio fischeri* for symbiont partner finding. *Physical Review Research*, 6(3):033214, 2024.
- [38] A. L. Schaefer, B. L. Hanelka, A. Eberhard, and E. P. Greenberg. Quorum sensing in *vibrio fischeri*: probing autoinducer–luxr interactions with autoinducer analogs. *Journal of Bacteriology*, 178(10):2897–2901, 1996.
- [39] C. Lupp, M. Urbanowski, E. P. Greenberg, and E. G. Ruby. *Vibrio fischeri* uses two quorum-sensing systems for the regulation of early and late colonization factors. *Journal of Bacteriology*, 187(11):3620–3629, 2005.
- [40] Alys Jepson, Vincent A. Martinez, Jana Schwarz-Linek, Alexander Morozov, and Wilson C. K. Poon. Enhanced diffusion of nonswimmers in a three-dimensional bath of motile bacteria. *Physical Review E*, 88(4):041002, 2013.
- [41] Johannes Taktikos, Holger Stark, and Vasily Zaburdaev. How the motility pattern of bacteria affects their dispersal and chemotaxis. *PLoS ONE*, 8(12):e81936, 2013.
- [42] Deborah S. Millikan and Edward G. Ruby. Alterations in *vibrio fischeri* motility correlate with a delay in symbiosis initiation and are associated with additional symbiotic colonization defects. *Applied and Environmental Microbiology*, 68(5):2519–2528, 2002.
- [43] J. Graf, P. V. Dunlap, and E. G. Ruby. Effect of transposon-induced motility mutations on colonization of the host light organ by *vibrio fischeri*. *Journal of Bacteriology*, 176(22):6986–6991, 1994.

# Supplementary Information

Chunhe Li, Zixiang Lin, Hongyi Bian, Anqi Li, Honyi Xin, Zijie Qu

## 1 Materials and methods

### 1.1 Cell culture

*Vibrio fischeri* cells (strain CICC24882) used in the experiments are obtained from the China Industrial Microbial Culture Collection and Management Center (CICC). The cells are cultured in Marine Broth 2216E in 250 mL Erlenmeyer flasks sealed with gas-permeable membranes, which allow sufficient gas exchange while minimizing external perturbations. Cultures are maintained at 16 °C. Cells are first grown in Marine Broth 2216E for approximately 24 h and subsequently diluted 1:500 into fresh media, followed by an additional 6–8 h of growth prior to experiments. At this stage, cells exhibit stable swimming behavior and high viability, ensuring consistent experimental conditions.

### 1.2 Sample preparation

After cultivation, *V. fischeri* cells are gently transferred into TMN motility buffer (Tris–HCl-based buffer containing NaCl, MgCl<sub>2</sub>, and glucose) for swimming behavior observations. TMN provides a well-defined ionic and energetic environment that sustains motility while suppressing uncontrolled growth during measurements (Table 1).

For experiments involving complex fluids, polyvinylpyrrolidone (PVP,  $M_w \approx 360$  kDa) and/or Methocel (methylcellulose) are added to TMN at prescribed concentrations expressed as weight/volume percentages (% w/v), depending on the experimental objective. Following polymer addition, the solutions are mixed on an orbital shaker at 200 rpm for more than 12 h to ensure complete polymer dissolution.

Table 1: Composition of TMN motility buffer (1×) per liter

Component	Chemical formula	Amount per 1 L
Tris–HCl buffer	–	50 mM
Sodium chloride	NaCl	17.5 g
Magnesium chloride (anhydrous)	MgCl <sub>2</sub>	0.48 g
D-Glucose	C <sub>6</sub> H <sub>12</sub> O <sub>6</sub>	0.90 g
Deionized water	–	to 1 L

### 1.3 Bioluminescence imaging setup

Quorum-sensing-induced bioluminescence is monitored using an industrial CMOS camera (model MV-CU120-10UC) operated in continuous acquisition mode. Image acquisition and camera control are performed using the manufacturer-provided machine vision software (HIKROBOT MVS, version 4.5.1). A fixed-focus lens (MVL-HF0624M-10MP) is mounted to provide a stable field of view and high light-collection efficiency.

All measurements are conducted in a light-tight darkroom to eliminate background illumination. The imaging system is maintained at a constant temperature of 16 °C throughout the experiment to ensure stable physiological conditions. Time-lapse images are recorded at a temporal resolution of one frame per minute, enabling continuous tracking of the onset and temporal evolution of bacterial bioluminescence.

The cell concentration is then quantified using optical density measurements at 600 nm (OD<sub>600</sub>). After concentration calibration, the samples are placed in a dark environment, where the bioluminescence emitted by the bacterial population is recorded. Bioluminescence is monitored by time-lapse imaging, and the recorded images are converted to 8-bit grayscale format, with pixel intensities ranging from 0 to 255. The average grayscale intensity is used as a quantitative measure of bioluminescence output, allowing consistent comparison across different fluid conditions. The results are summarized in Fig. S1. The bioluminescence intensity increases monotonically with cell concentration, demonstrating a clear positive correlation between QS-activated light emission and population density. In contrast, the duration of the luminescence signal decreases as the cell concentration increases. This inverse relationship is likely due to rapid depletion of dissolved oxygen at high cell densities, which limits the sustainability of the bioluminescent reaction.

#### 1.4 3D real-time tracking technology

3D real-time tracking technology was used to record the three-dimensional swimming trajectory of individual *V. fischeri* for a long time. The cells were viewed by using an inverted microscope model Nikon ECLIPSE Ti2-U with PX.EDGE 5.5-sCMOS camera. A two-dimensional displacement stage was used to track the movement of cells in the direction of parallel glass plates. The piezoelectric displacement stage (Pi) was used to record the movement of the cells in the vertical direction and control the position of the focal plane to ensure that the cells were always in view. Through the algorithm written by C++ language, the images were obtained at 60fps, 300X300 pixels. And the data of the two-dimensional and the piezoelectric displacement stage were recorded at the same time. The real-time three-dimensional motion trajectory of the cell was finally obtained in the specified time. As shown in Fig. S2, each cell is continuously tracked for a duration of 10 s, allowing the entire run–pause–reverse swimming cycle of each cell to be clearly resolved.

#### 1.5 Fluid rheological properties

To investigate how fluid viscosity and rheological properties influence quorum-sensing (QS)-activated bioluminescence in *V. fischeri*, we systematically vary the physical properties of the surrounding media. Two representative polymers are employed to separately examine the effects of increased viscosity and those associated with non-Newtonian rheology. The rheological properties of these polymer solutions are characterized over a broad range of shear rates (Fig. S3). As shown in Fig. S3A, PVP360k solutions exhibit an approximately shear-rate-independent viscosity across the measured range, indicating that the fluid retains a nearly constant viscosity even at higher polymer concentrations. In contrast, Methocel solutions exhibit pronounced shear-thinning behavior, with viscosity decreasing as the shear rate increases (Fig. S3B). For selected concentrations, PVP360k and Methocel solutions are adjusted to have comparable viscosities in the low-shear regime relevant to bacteria swimming, allowing a direct comparison between Newtonian and non-Newtonian fluids with similar viscous resistance but different rheological behavior.

## 2 Analysis of the resistive force theory of *V. fischeri*

We propose that the experimentally observed slowdown of *V. fischeri* in Methocel-containing motility buffer arises from the influence of viscoelastic stresses on flagellar propulsion [1]. As shown in Fig. S4A, in Newtonian fluids, the rotation of the flagella generates thrust that balances the hydrodynamic

Table 2: Typical geometric parameters used in cell swimming calculations [2].

Symbol	Description	Value
$a$	Cell length	1.70 $\mu\text{m}$
$b$	Cell width	0.79 $\mu\text{m}$
$l$	Flagellum length	4.20 $\mu\text{m}$
$p$	Flagellum pitch	2.40 $\mu\text{m}$
$R$	Flagellum helix radius	0.27 $\mu\text{m}$
$r_0$	Flagellum filament radius	0.05 $\mu\text{m}$

resistance on the cell body, leading to stable forward motion. In contrast, in the viscoelastic Methocel buffer, the rapid rotation of the flagella generates elastic stresses in the surrounding polymer network, resulting in additional resistance that reduces propulsion efficiency. Resistive Force Theory (RFT) is used to analyze the motor drive characteristics. In RFT, the dynamical characteristics of the cell are determined by the geometric properties of the cell body and flagella, and the geometric parameters used in the calculations are summarized in Table 2. As shown in Fig. S4B, the motor torque decreases with increasing rotation frequency, indicating a non-constant torque-speed characteristic. This hydrodynamic response leads to a viscosity-dependent reduction in the motor rotation rate, while the corresponding propulsive thrust force increases moderately with viscosity due to enhanced viscous resistance (Fig. S4C).

### 3 Derivation of the effective diffusion coefficient

Within a time window  $t$ , the cell undergoes approximately  $t/\tau_{\text{run}}$  reorientation events, each contributing a factor  $\langle \cos \theta \rangle$  to the decay of orientational memory. After  $t/\tau_{\text{run}}$  such events, the orientation autocorrelation function can be written as:

$$\langle \mathbf{e}(0) \cdot \mathbf{e}(t) \rangle = \exp \left[ -\frac{t}{\tilde{\tau}} \right], \quad \tilde{\tau} = \frac{\tau_{\text{run}}}{1 - \langle \cos \theta \rangle} \quad (1)$$

The corresponding velocity autocorrelation function then takes the form:

$$C(t_1, t_2) = v^2 \exp \left( -\frac{|t_2 - t_1|}{\tilde{\tau}} \right), \quad (2)$$

The mean square displacement can be obtained from the velocity autocorrelation function as:

$$\langle [\mathbf{r}(t) - \mathbf{r}(0)]^2 \rangle = 2v^2 \tilde{\tau}^2 \left( \frac{t}{\tilde{\tau}} - 1 + e^{-t/\tilde{\tau}} \right), \quad (3)$$

In a three-dimensional environment, when  $t$  is large enough, the ordinary diffusion satisfies:

$$\langle \Delta r^2(t) \rangle \approx 6Dt, \quad \langle [\mathbf{r}(t) - \mathbf{r}(0)]^2 \rangle \sim 6Dt \quad (4)$$

From this expression, the effective diffusion coefficient is obtained as:

$$D = \frac{v^2 \tau_{\text{run}}}{3(1 - \langle \cos \theta \rangle)}. \quad (5)$$

Analysis of the trajectory statistics shows that the distribution of run and wrap durations is well described by an exponential form (Fig. S5 and Fig. S6), supporting a Poisson description of reorientation events.

Fig. S7 summarizes the dependence of the Péclet number on viscosity for *V. fischeri* swimming in PVP360k and Methocel solutions. The Péclet number provides a dimensionless measure of the relative importance of directed swimming compared to diffusive spreading, and is defined as

$$Pe = \frac{u \ell}{D}, \quad (6)$$

where  $u$  is the mean swimming speed,  $D$  is the effective diffusion coefficient, and  $\ell$  is a characteristic length scale associated with cell motion. Physically, a large Péclet number indicates that directed swimming dominates transport over this length scale, whereas a small Péclet number implies that motion is largely diffusive. As shown in Fig. S7, the Péclet number varies only weakly with viscosity in both PVP360k and Methocel solutions. Over the viscosity range explored here, the values in the two buffers remain comparable, with no clear systematic separation between Newtonian and viscoelastic conditions.

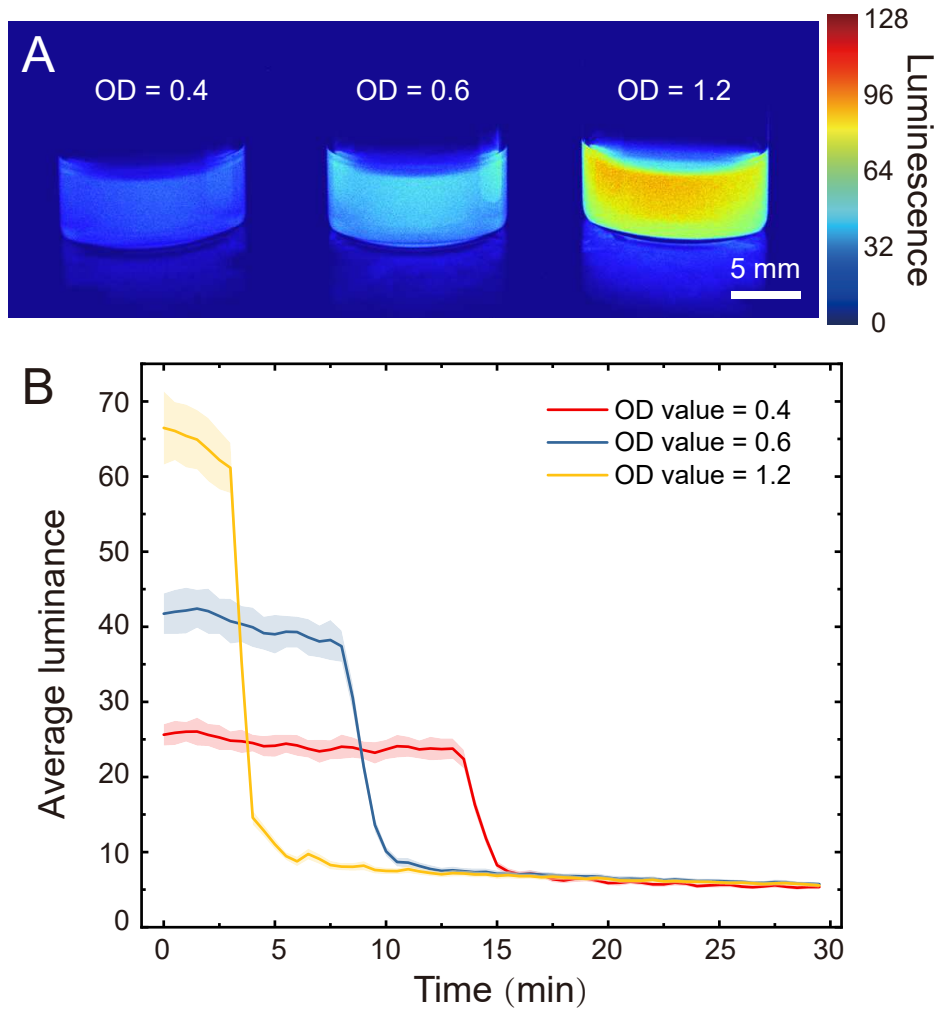


Figure S1. Dependence of quorum-sensing-activated bioluminescence on cell concentration. (A) Representative images of *V. fischeri* suspensions at different  $OD_{600}$  values. (B) Time evolution of the average luminescence, illustrating a positive correlation between peak intensity and cell concentration, accompanied by a reduced luminescence duration at higher densities.

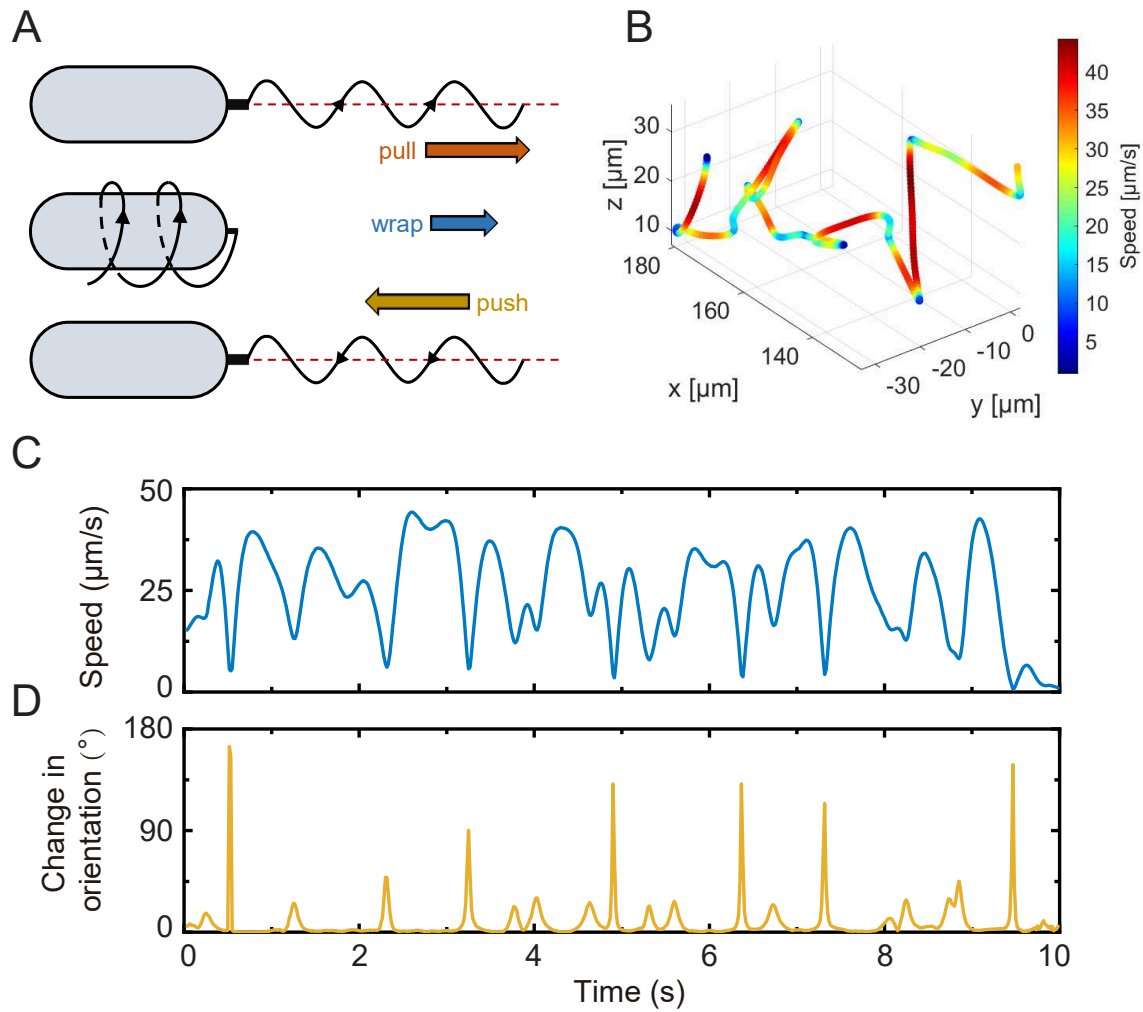


Figure S2. Three-dimensional tracking of *V. fischeri* swimming behavior. (A) Schematic illustration of the three characteristic motility modes of *V. fischeri*: push, pull, and wrap. (B) A representative three-dimensional trajectory displaying the characteristic run–pause–reverse behavior. (C,D) Wrap modes are associated with a pronounced reduction in swimming speed and large changes in swimming direction.

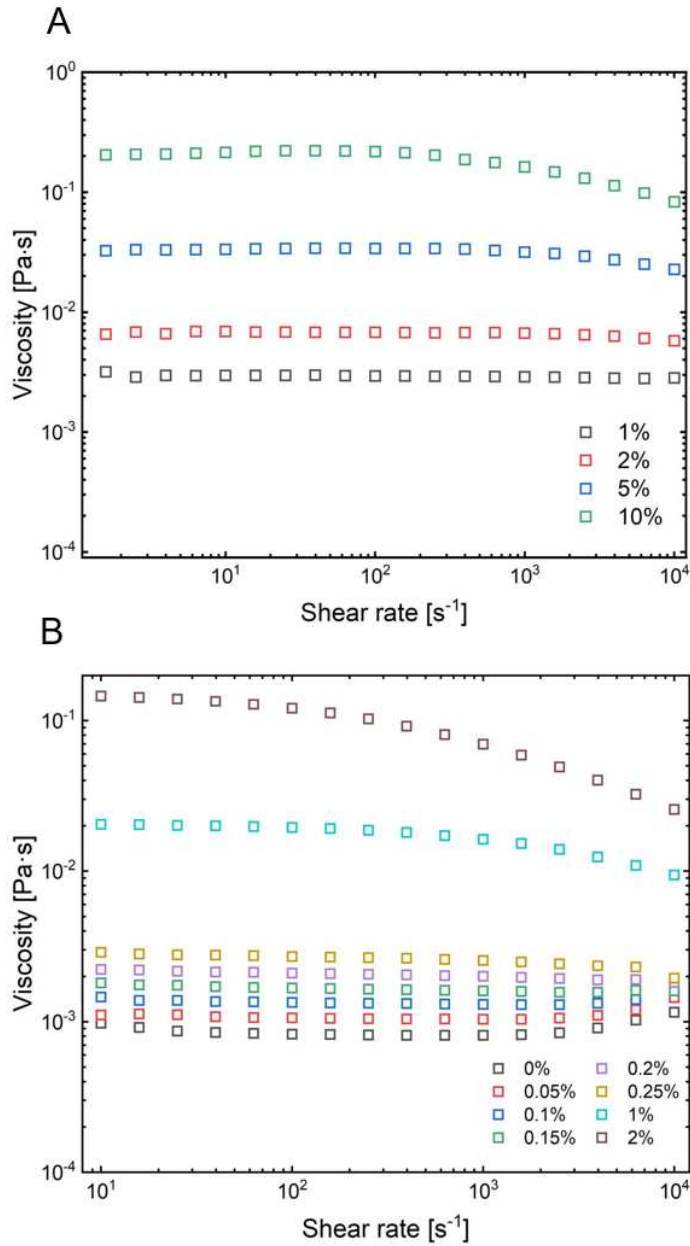


Figure S3. Rheological characterization of polymer solutions used in this study. Shear viscosity as a function of shear rate for (A) PVP360k solutions, exhibiting Newtonian behavior, and (B) Methocel solutions, displaying pronounced shear-thinning characteristics.

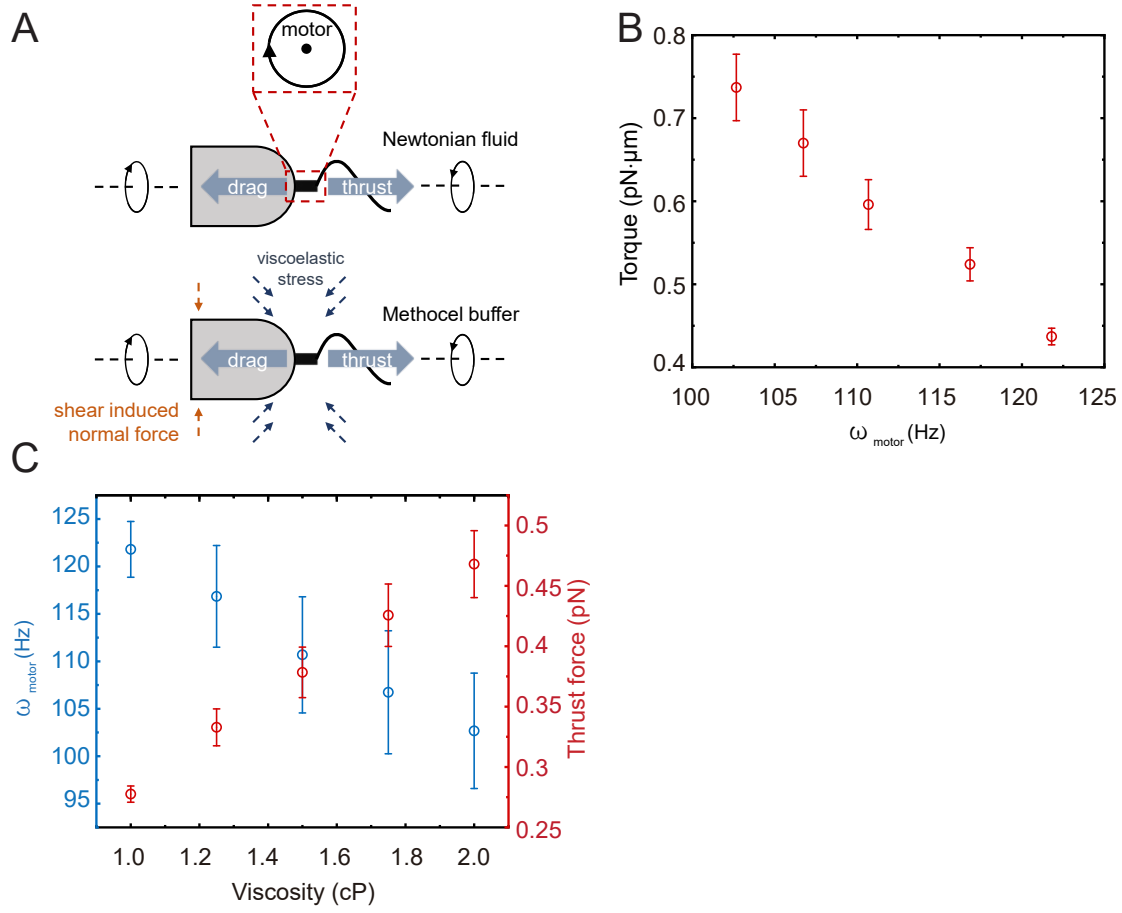


Figure S4. Hydrodynamic interpretation of viscosity-dependent swimming in *V. fischeri* based on resistive force theory (RFT) and viscoelastic corrections. (A) Schematic illustration of force balance during bacterial swimming in a Newtonian fluid (PVP360k-containing buffer) and a viscoelastic non-Newtonian fluid (Methocel-containing buffer). In Newtonian fluids, propulsion is governed by the balance between motor-generated thrust and viscous drag, whereas in Methocel solutions additional viscoelastic stresses act on the flagellum, reducing propulsion efficiency. (B) Motor torque as a function of motor rotation frequency  $\omega_{\text{motor}}$ , calculated using RFT with geometric parameters listed in Table 2. (C) Viscosity dependence of the motor rotation frequency  $\omega_{\text{motor}}$  (left axis) and the corresponding propulsive thrust force (right axis) predicted by RFT.

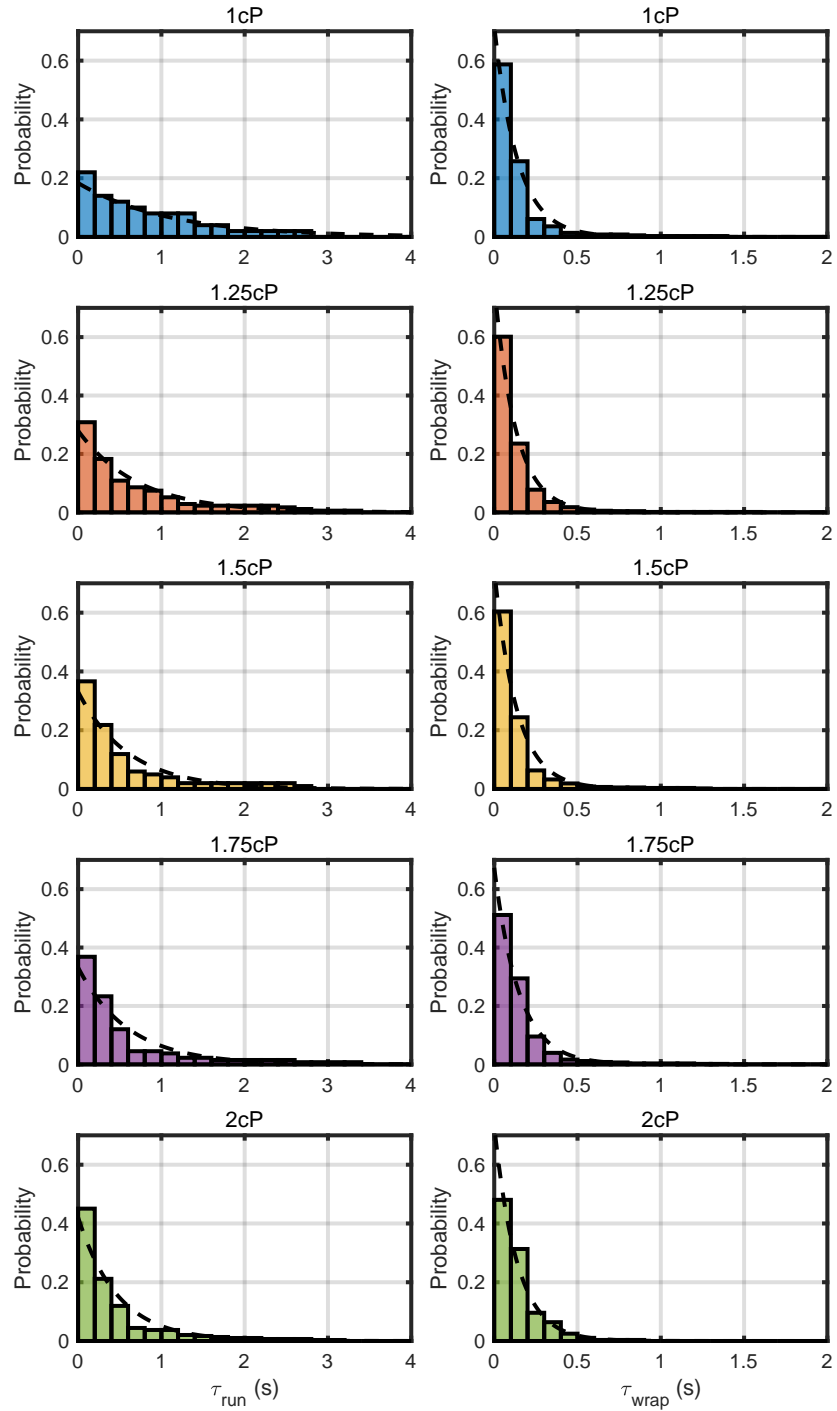


Figure S5. Probability distributions of run durations  $\tau_{\text{run}}$  (left) and wrap durations  $\tau_{\text{wrap}}$  (right) for *V. fischeri* swimming in PVP360k solutions at different viscosities. Dashed lines indicate exponential fits, showing that both run and wrap durations follow exponential statistics.

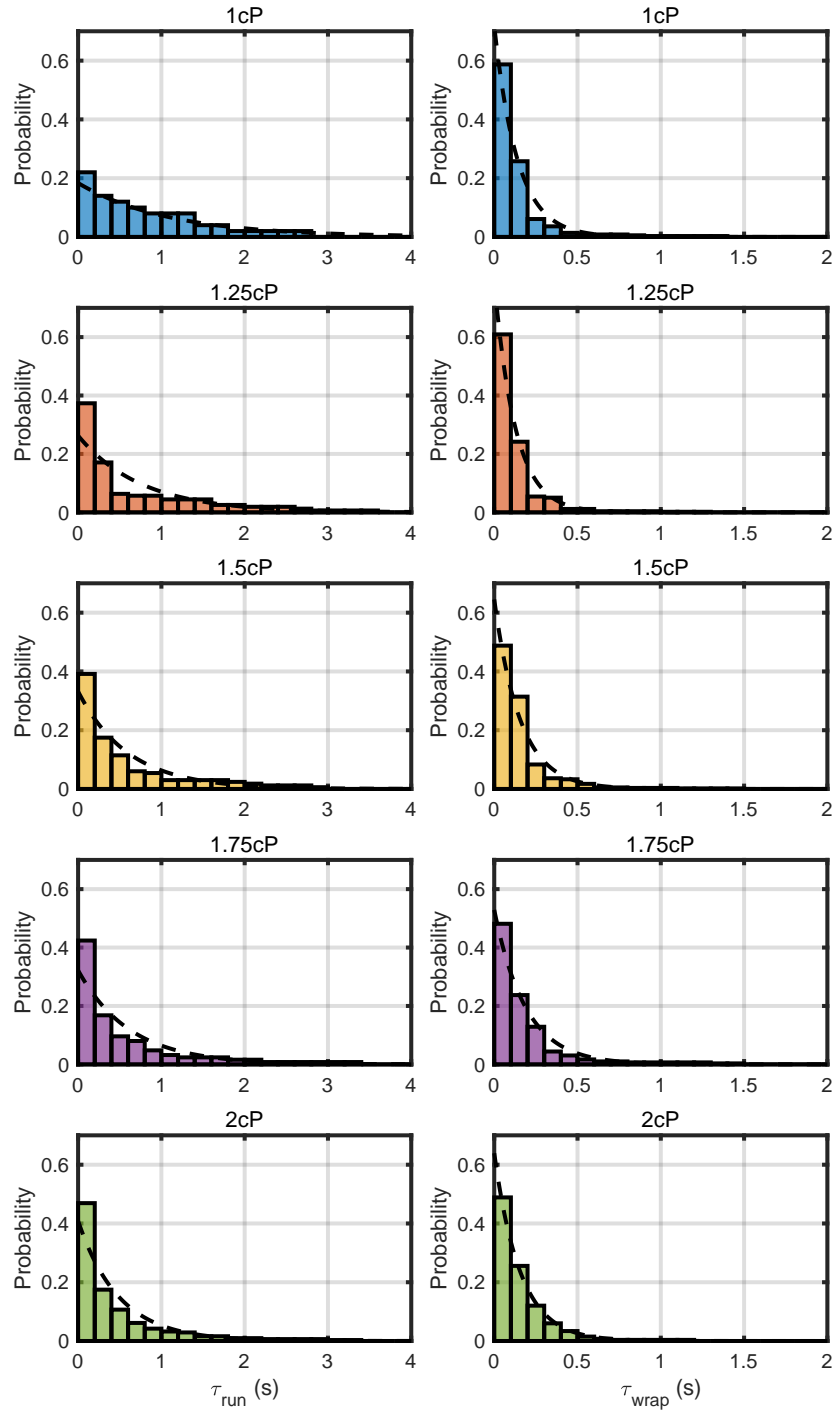


Figure S6. Probability distributions of run durations  $\tau_{\text{run}}$  (left) and wrap durations  $\tau_{\text{wrap}}$  (right) for *V. fischeri* swimming in Methocel solutions at different viscosities. Dashed lines represent exponential distributions of both run and wrap durations.

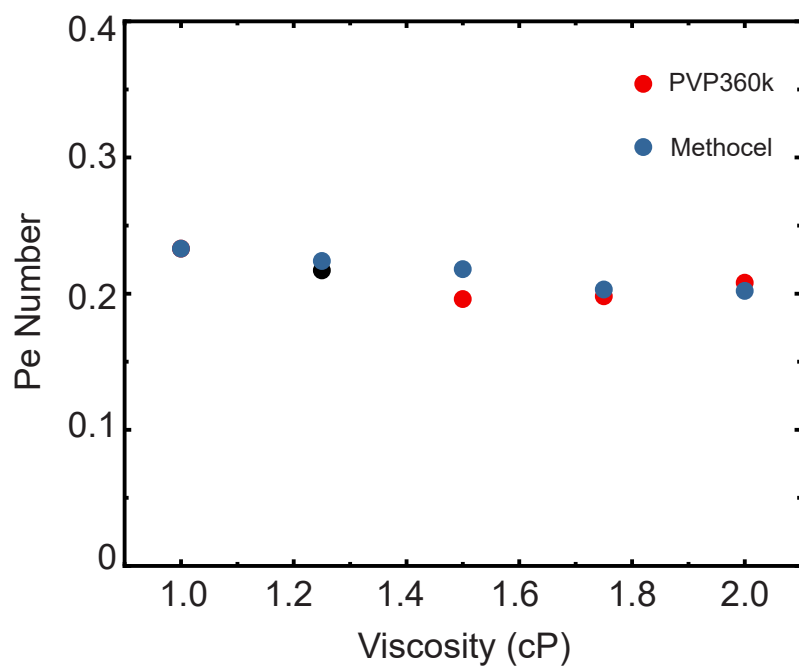


Figure S7. Viscosity dependence of the Péclet number in Newtonian and viscoelastic media.

## References

- [1] Yukio Magariyama and Seishi Kudo. A mathematical explanation of an increase in bacterial swimming speed with viscosity in linear-polymer solutions. *Biophysical Journal*, 83(2):733–739, 2002.
- [2] Yoshiaki Kinoshita, Yoshitomo Kikuchi, Nagisa Mikami, Daisuke Nakane, and Takayuki Nishizaka. Unforeseen swimming and gliding mode of an insect gut symbiont, *burkholderia* sp. rpe64, with flagella wrapping around its cell body. *The ISME Journal*, 12(3):838–848, 2018.

Caption for Movie S1. 3D real-time tracking of *V. fischeri* in a motility buffer with a viscosity of 1 cP

Caption for Movie S2. 3D real-time tracking of *V. fischeri* in a PVP360k containing motility buffer with a viscosity of 1.5 cP

Caption for Movie S3. 3D real-time tracking of *V. fischeri* in a PVP360k containing motility buffer with a viscosity of 2 cP

Caption for Movie S4. 3D real-time tracking of *V. fischeri* in a Methocel containing motility buffer with a viscosity of 1.5 cP

Caption for Movie S5. 3D real-time tracking of *V. fischeri* in a Methocel containing motility buffer with a viscosity of 2 cP

Caption for Movie S6. Quorum-sensing activated bioluminescence in *V. fischeri*